Easy mass production of homogenous and uniform 3D spheroids for high-throughput screening applications

Marco P. Leu[*], Natacha Calatayud[*], Francis Smet[†], Angela Comas[†], Andreas Thomsen[‡]

ABSTRACT

To have a predictive and reliable 3D cell culture tool at hand to run successful high-throughput screening projects is the challenge of our days. Past drug discoveries from 2-dimensional assays have shown intolerable failure rates in preclinical trials. With 3D CoSeedis™, abc biopply now presents a novel and unique 3D cell culture platform for easy mass production of homogeneous and uniform 3D spheroids that feeds seamlessly into current screening processes. Mass produced spheroids can efficiently and accurately be distributed in HTS compatible plate formats using COPAS VISION™ large particle flow cytometer (Union Biometrica, Inc). In addition to standard flow cytometry parameters the COPAS VISION captures in-flow bright field images of the spheroids.

INTRODUCTION

High-throughput screening (HTS) methods based on 2-dimensional (2D) cell culture technologies have become a widely used approach in the discovery of new drugs (Ocana et al. 2010). However, a vast majority of the identified candidates originating from 2D screening assays fail in subsequent preclinical tests, and only a tiny fraction of compounds finally succeeds in clinical test phases, while the remaining drugs tested do not meet their primary endpoints (Harrer et al. 2019; Lee et al. 2018). To improve screening efficiency, hence reduce failure rates in identifying candidates at later clinical trial stages, it is eminent to develop screening applications that are closer to the biological environment, in which the compound eventually acts. 3-dimensional (3D) cell culture technologies have become one of the major foci in this respect since numerous studies indicated that cells grown in 3D show a physiologically more relevant response to applied test compounds (Walzl et al. 2014; Kochanek et al. 2020; Brandenberg et al. 2020), which is consequently expected to increase the predictiveness of clinical trial results (Li and LaBarbera 2017).

Despite the pharmacological (Ryan et al. 2016) and biological (Courau et al. 2019; Kondo et al. 2019) benefits of 3D cell systems, there are also some substantial challenges in the implementation of 3D constructs in HTS assays: a) poor reproducibility of 3D structures (Das et al. 2016), b) labour intensiveness, c) overcomplicated systems, d) inability to upscale, e) difficulties in recovering

[*] abc biopply ag, Switzerland
[†] Union Biometrica, Inc., USA
[‡] Universitätsklinikum Freiburg, Germany

cultures, f) incompatibility with automated systems, g) lack of flexibility, h) more complex imaging requirements (e.g. confocal microscopy as shown by Tijmen H. Booij et al. 2019, and i) long-term stability problems have been the main reasons invoked against the use of 3D cultures in drug screening setups (Ryan et al. 2016).

abc biopply has developed a 3D culture technology named 3D CoSeedis™ that, in combination with Union Biometrica's COPAS VISION™, eliminates those drawbacks and makes 3D cultures accessible for efficient and upscalable high-throughput compound screening.

The results demonstrate the unprecedented advantages 3D CoSeedis™ offers as a tool of mass production for 3D cell cultures. Using COPAS VISION™ for spheroid sorting (Union Biometrica, Inc., USA), the resulting homogenously seeded 384-well plates are perfectly compatible with current standard screening protocols.

MATERIALS AND METHODS

Cell lines and 2D cell culture

Five different cell lines (CLS Cell Lines Service GmbH, Eppelheim, Germany) were used: (1) HT-29, (2) WiDr, (3) BT-474, (4) A-549 and (5) LNCaP. Cell culture experiments were performed working under a laminar flow hood. All solutions were pre-warmed in a water bath at 37°C prior to contact with cells. 3D CoSeedis™ Aggregation Media (abc biopply ag, Solothurn, Switzerland) for WiDr, LNCaP, A-549, HT-29 and BT-474 were used, respectively. Those media were supplemented with either 5% for 2D or 3% for 3D cell growth with: (1) human AB-Serum (Cellovations®, PELOBIOTECH GmbH, Planegg, Germany) or (2) fetal calf serum (FCS) (Bioconcept AG, Allschwil, Switzerland), respectively. Cells were thawed and seeded in 75 cm^2 or 25 cm^2 cell culture flasks, respectively. Subsequently, they were transferred into a cell culture incubator at 37°C, 5% CO_2 and 90% humidity until they reached 60-80% confluency. To split and expand cells, they were washed with Dulbecco's PBS without Ca^{2+}/Mg^{2+} (PBS), detached with Cell Passaging Solution (Accutase) (Cellovations®, PELOBIOTECH GmbH, Planegg, Germany) for 8-10 minutes at room temperature (RT) and diluted in 10 mL medium. Subsequently, a centrifugation at 300 g for 3 to 5 minutes, was followed by a re-suspension of the pellet in medium. According to the cell count in a disposable hemocytometer, cells were seeded at the appropriate ratio in 75 cm^2 cell culture flasks. Medium was changed regularly every 2-3 days.

3D CoSeedis™

3D CoSeedis™ Chip680s (abc biopply ag, Solothurn, Switzerland) were equilibrated in 1 mL of corresponding medium in 24-well plates (CELLSTAR®, Greiner Bio-One GmbH, Kremsmünster, Austria), centrifuged at 200 g for 3-5 minutes and stored overnight in the incubator prior to cell seeding. Once the expanded cells reached 60-80% confluency in the flasks, they were detached and collected as described above. After resolving the cell pellet in medium, the resulting suspension was passed through a cell strainer (40 µm pore size). Cell density in the suspension was determined by the use of a hemocytometer. After having removed the medium of 3D CoSeedis™ Chip680, 100 cells per microwell (cpm) were seeded according to manufacturer's instructions (abc biopply ag, Solothurn, Switzerland).

The passage number of each cell line at the time of seeding was: p51 for HT-29, p56 for WiDr, p40 for BT-474, p17 for A-549 and p57 for LNCaP. After seeding, 24-well plates were left under the hood for at least 20 minutes to allow cells to sediment. Subsequently, they were transferred to the incubator overnight for 3D aggregation. The next day, all 3D CoSeedis™ Chip680s were transferred to new 24-well plates containing fresh medium with 3% supplement to avoid possible 2D cell growth underneath the 3D CoSeedis™ chips. The cells were incubated in 3D CoSeedis™ Chip680 for 5-9 days. Medium was changed regularly every 2-3 days.

Harvesting of 3D cell cultures

Fully aggregated spheroids were collected by replacing the medium with PBS. All 3D CoSeedis™ Chip680s were subsequently flipped upside-down. Centrifugation at 300 g for 30 seconds released all spheroids from the microwells of 3D CoSeedis™ Chip680, which was subsequently removed and the spheroid-suspension was collected in a conical 50 mL centrifuge tube. Simultaneously, 384-well plates (spheroid microplate; Corning Incorporated, New York, USA) were pre-filled with 22 uL of the corresponding medium.

COPAS VISION™ analysis

3D cultures were sorted, imaged and analyzed using a COPAS VISION™ (Union Biometrica Inc., Massachusetts, USA), for handling objects ranging between 10 and 400 µm according to the manufacturer's instructions. Samples were analyzed with a single 488 nm solid state laser and gated by time-of-flight (relative size) vs. extinction (optical density) to exclude possible cell debris or polyspheroidal structures. In-flow bright-field images were taken of the gated spheroids prior to being sorted dropwise (3 uL) into individual wells of a 384-well plate pre-filled with media. Post-sorting, images were processed to determine area, circumference, roughness and mean greyscale.

Viability Assay

Cell viability was assessed of all spheroids after sorting in 384-well plates using the CellTiter-Glo® 3D Viability Assay (Promega Corporation, Madison, USA). 384-well plates with one spheroid per well were treated as described in the manufacturer's instructions. Half of the sorted 384-well plates were used to perform the assay immediately (D0) and luminescence was determined using an integration time of 1 second (GloMax® Discover GM3000, Promega Corporation, Madison, USA). The other half of the plates were kept for 2 days in the incubator before the assay was performed under identical integration settings (D2). The viability assay with medium and supplement only resulted in no significant luminescence (blank, determining baseline for non-specific luminescence). Plates with CellTiter-Glo® 3D Reagent added showed an increase in luminescence levels indicating the presence of liable spheroids. In contrast, spheroids that were treated similarily but included cell toxins showed the expected decrease in luminescence signal (data not shown).

RESULTS

Preparing a suspension of homogenous and uniform spheroids with 3D CoSeedis™

3D CoSeedis™ chips consist of an agarose-based carrier matrix that allows the cultivation and aggregation of cells in a flexible and reproducible manner resulting

in up to 16’320 3D cultures per 24-well plate. Seeding of a 3D CoSeedis™ chip is shown schematically in Figure 1.

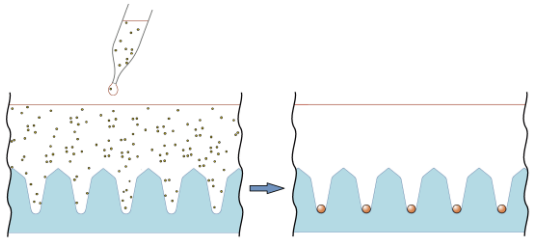

Figure 1: Loading of 3D CoSeedis™ chips with cells. By sedimentation, cells assemble at bottom of conical microwells, where one spheroid per microwell is formed.

The system is based on a modular design that allows co-cultivation of feeder cells, either in distance to or in contact with the actual test cells. Manipulation, cultivation, and harvesting of fully grown 3D cultures is simple and robust resulting in a highly homogenous and uniform population of either spheroidal or conical 3D cultures (Thomsen et al. 2017). Figure 2 shows a representative group of harvested HT-29 and BT-474 spheroids suspended in 1xPBS w/o Mg^{2+}/Ca^{2+}.

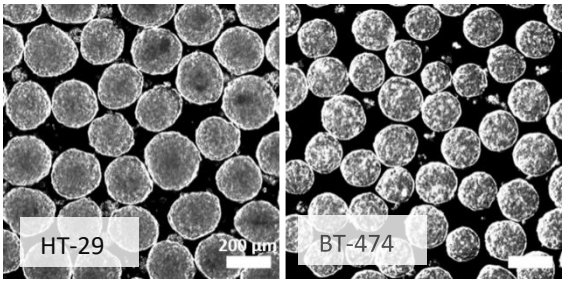

Figure 2: Micrographs of 3D cultures harvested from 3D CoSeedis™. Spheroids were fixed in 4% formalin after harvesting. Cell lines as indicated.

3D CoSeedis™ allows the harvesting of > 65,000 3D cultures in a single short centrifugation step with the ability to scale up (schematic representation of 3D CoSeedis™ chips during harvesting in Figure 3).

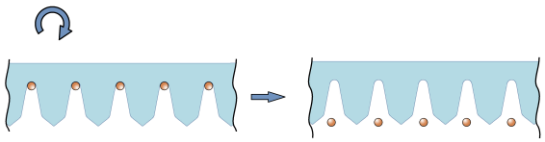

Figure 3: Spheroid harvesting. Due to the conical shape of microwells, spheroids are easily released by centrifugation.

Separation of 3D cell cultures and seeding of 384-well plates

The obtained suspension of 3D cultures was subsequently dispensed into an HTS-compatible multi-well plate, e.g. 384-well plates, resulting in separated, single spheroids per well. The automated dispensing, bright field image capture, and analysis of the 3D cultures was done using Union Biometrica’s COPAS VISION™ large particle flow cytometer. A scheme of the sorting process is shown in Figure 4.

The COPAS VISION™ is based on the fundamental principles of flow cytometry, but differs from traditional flow cytometers in several important design areas: Firstly, the large-bore fluidics of COPAS VISION™ instruments can accommodate objects as wide as 10–750 µm, a range that is much larger than traditional flow cytometers. Secondly, COPAS VISION™ systems operate at slower flow rates and lower pressures, thereby avoiding potentially disruptive high shear forces inherent in standard flow cytometers.

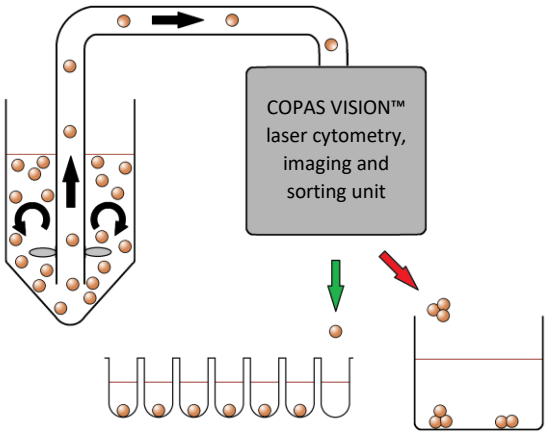

Figure 2: Schematic representation of spheroid sorting principle. Spheroids are kept in suspension by gentle stirring. Suspended spheroids are driven towards the COPAS VISION™ sorting unit by applying a slight overpressure in the suspension tube. Spheroids are subsequently gated depending on the preset parameters. Particles matching the size criteria were dispensed into a 384-well plate (green arrow) at a fixed number of spheroids per well, while ungated spheroids, aggregates, and debris are discarded into a separate compartment (red arrow).

The third difference is the heart of the COPAS VISION™ technology: a patented pneumatic sorting mechanism, located downstream of the flow cell, utilizes an air diverter to dispense organisms and large cells in a fluid drop. In contrast, traditional cytometers typically rely on mechanical sorting or application of a large electrostatic charge. Both of these have limitations when large particle samples are involved.

For monitoring, analysis, and documentation purposes, gated spheroids were photographed using the instrument's capability to take in-flow bright-field images prior to the sorting into individual wells of a 384-well plate. Besides the spheroid, sorting also dispenses a volume of approximately 3 µl of PBS w/o Mg^{2+}/Ca^{2+} per well. Each well was initially pre-filled with 22 µl of medium for subsequent viability testing and incubation. Examples of in-flow photographs of HT-29, WiDr, LNCaP, BT-474, and A-549 spheroids, respectively, are show in Figure 5 and 6. In addition, Figure 5 also shows the full range of images the COPAS VISION™ is capturing for each sorted 384-well plate, giving full traceability of individual spheroids. Images were further processed to determine cross section area, circumference, and roughness or roundness of each spheroid. Simultaneously, the "time of flight" (time required for a spheroid to pass through the laser beam of each gated spheroid was measured as an indicator of spheroidal shape and size (see Table 1).

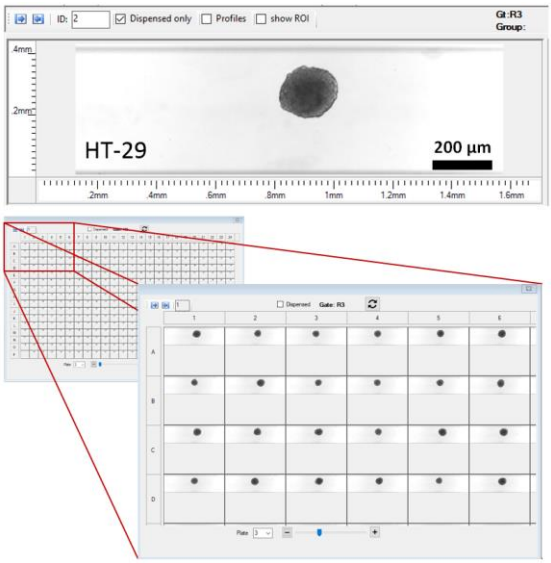

Figure 3: Different image details of brightfield images of HT-29 spheroids in-flow. For each well, COPAS VISION™ provides the image of the sorted spheroid.

In this study, we dispensed exactly 1 spheroid per well of the 384-well plate. Sorting took less than 5 minutes per 384-well plate, which equals an average sorting speed of a little more than 1 spheroid per

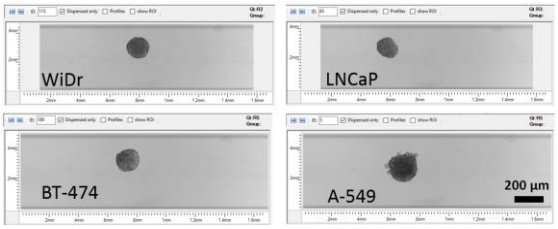

Figure 4: Bright-field images of spheroids in-flow. Cell lines as indicated.

second. Figure 7 shows different spheroids in a 384-well plate after sorting.

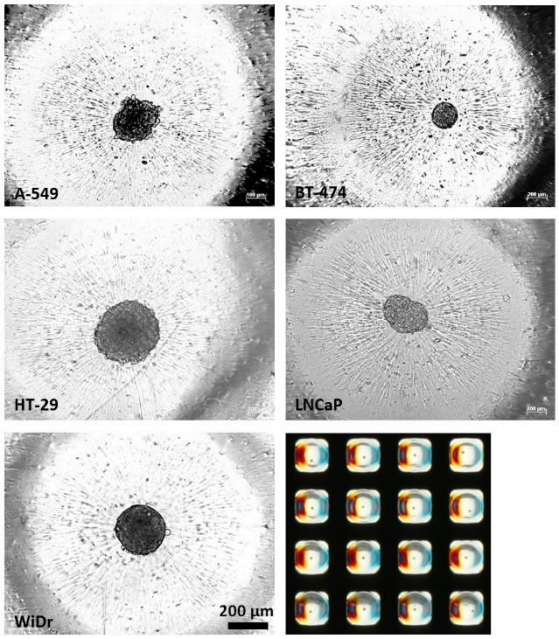

Figure 5: Micrographs of single spheroids sorted into 384-well plates. Lower right: section of a 384-well plate with sorted spheroids, transmitted light scan.

The probability of a misfilled well (either empty or more than one 3D culture per well) was below 2%.

Each type of spheroids analysed in this study resulted in 384-well plates seeded with a very homogenous population of spheroids. The average size of spheroids per plate differed as little as 0.01% in TOF (standard error of the mean (SEM)). Table 1 shows TOF, cross section area, circumference, and image roughness/roundness of all different spheroid types analysed. Size discrepancies according to TOF range between 0.01% (A-549, D2) and 1.54% (LNCaP, D2) depending on cell type and gating stringency. The homogeneity among 3D cultures generated by 3D CoSeedis™ leads to a highly efficient sorting process in the COPAS VISION™ minimizing both, setup time and wasted 3D cultures. Furthermore, it reduces the initially required cell culture time by considerably minimising the

		HT-29				WiDr			
		TOF [x 0.2 µs]	**Cross section area** [um^2]	**Circumference** [µm]	**Img. Roughness/Roundness** [Area / Circumference x Const.]	**TOF** [x 0.2 µs]	**Cross section area** [um^2]	**Circumference** [µm]	**Img. Roughness/Roundness** [Area / Circumference x Const.]
D0	AVG	751.61	26420.23	570.99	598.23	700.93	23255.81	618.88	715.15
	STD	3.25	474.87	13.99	11.49	5.09	1987.66	45.07	67.42
	SEM	0.43%	1.80%	2.45%	1.92%	0.73%	8.55%	7.28%	9.43%
D2	AVG	759.31	35226.11	731.45	826.54	n.d.	n.d.	n.d.	n.d.
	STD	2.56	315.64	11.00	26.48	n.d.	n.d.	n.d.	n.d.
	SEM	0.34%	0.90%	1.50%	3.20%	n.d.	n.d.	n.d.	n.d.
		BT-474				**A-549**			
		TOF [x 0.2 µs]	**Cross section area** [um^2]	**Circumference** [µm]	**Img. Roughness/Roundness** [Area / Circumference x Const.]	**TOF** [x 0.2 µs]	**Cross section area** [um^2]	**Circumference** [µm]	**Img. Roughness/Roundness** [Area / Circumference x Const.]
D0	AVG	510.32	18576.10	519.42	847.49	643.98	22365.46	639.16	671.63
	STD	1.63	236.16	5.09	0.02	4.38	1703.16	42.49	23.38
	SEM	0.32%	1.27%	0.98%	0.00%	0.68%	7.62%	6.65%	3.48%
D2	AVG	510.24	18472.51	518.35	846.76	647.31	23721.31	681.21	639.74
	STD	2.40	221.23	2.05	3.06	0.10	368.46	6.14	5.04
	SEM	0.47%	1.20%	0.40%	0.36%	0.01%	1.55%	0.90%	0.79%
		LNCaP							
		TOF [x 0.2 µs]	**Cross section area** [um^2]	**Circumference** [µm]	**Img. Roughness/Roundness** [Area / Circumference x Const.]				
D0	AVG	633.71	26970.64	646.37	803.78				
	STD	10.43	24.43	1.67	4.23				
	SEM	1.65%	0.09%	0.26%	0.53%				
D2	AVG	646.04	27125.47	646.64	806.86				
	STD	9.96	335.55	4.79	2.19				
	SEM	1.54%	1.24%	0.74%	0.27%				

Table 1: In-flow images acquired of each gated and subsequently sorted spheroid were analysed for size and shape. The following parameters were captured: (1) time of flight (arbitrary value for the time it takes the spheroid to travel through the laser beam vs. extinction of the object – indicative of relative size of object); (2) cross section area of spheroid based on image analysis; (3) circumference; (4) image roughness/roundness calculated as the ratio of the cross section area divided by its circumference. Shown are the averaged values of two 384-well plates per cell type. AVG: average; STD: standard deviation; SEM: standard error of the mean; TOF: time of flight; Img.: image

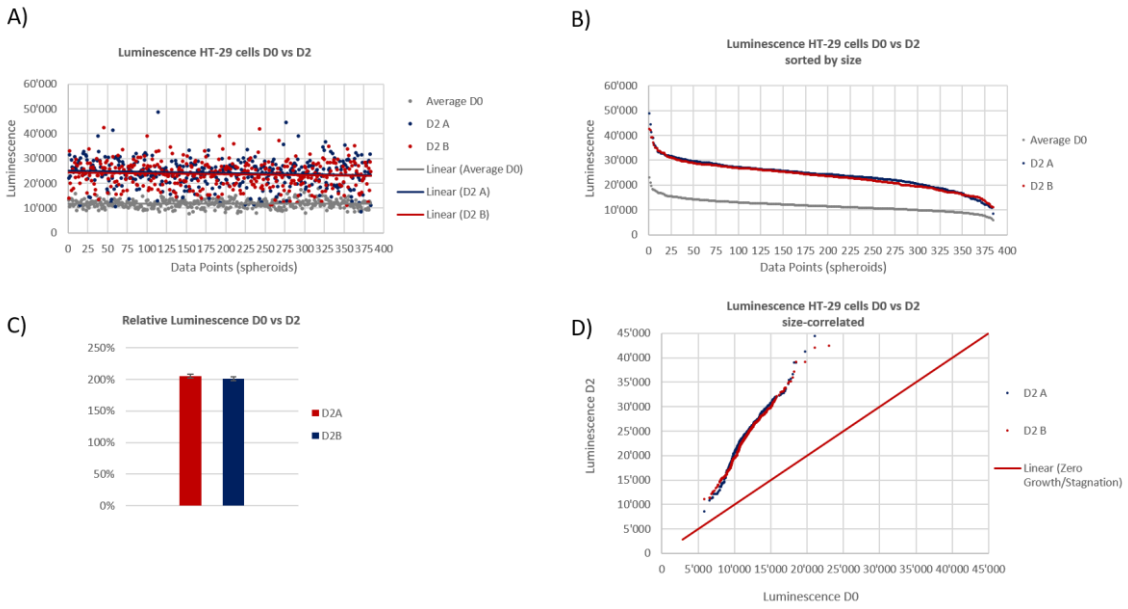

Figure 8: CellTiter-Glo® 3D Viability Assay on separated HT-29 (colon tumour) spheroids. A) Luminescence of individual wells at day 2 (D2) after separation were plotted (blue and red dots; in duplicates). Values at day 0 (D0) were averaged from two individual 384-well plates (grey dots). B) The same measurements were plotted but size arranged according to the intensity levels of luminescence. C) Relative luminescence of D2 vs. D0 of two individual sorted 384-well plates. Values at D2 were divided by the average of two 384-well plates at D0. Errors indicate SEM. D) Size-correlated representation of luminescence. Diagonal red line indicates zero growth (= stagnation). Data points above red line indicate positive growth, while data points below equal negative growth (= cell death).

number of 3D CoSeedis™ chips needed to generate enough spheroids for the sorting. In the current test series, 3D aggregation took less than 10 days to generate a total of approximately 180,000 spheroids at day 0 of the sorting. Furthermore, the initial setup time to start the sorting process was less than an hour with no additional further corrections.

Viability of separated 3D cultures

To address the question whether the sorting process had a negative effect on cell survival, cell viability was assessed on sorted 3D cultures. In a first analysis, luminescence values were plotted from both, day 0 (D0) and day 2 (D2) after separation. As an example, the values for HT-29 are shown in Figure 8A. A linear trend line was approximated to indicate the increase in luminescence, hence cell growth. Next, the same luminescence values were plotted, but this time they were arranged according to their intensity to get a clearer indication of the increase in luminescence between D0 and D2. Values for HT-29, WiDr, BT-474, A-549 and LNCaP are shown in Figure 8B and 9B, respectively. All cell types analysed showed an increase in luminescence from D0 to D2 (Figure 8, 9 and data not shown).

Furthermore, the increase in relative luminescence (Figure 8C and 9A) correlated with the expected growth rate for those spheroids. Based on this data, we argued that with the relative luminescence increasing as expected, the data could also be represented in a size-correlated manner. In such a graph, we would put small luminescence values at D0 in correlation with small values at D2 and large values at D0 with large values at D2, respectively, assuming that all 3D cultures

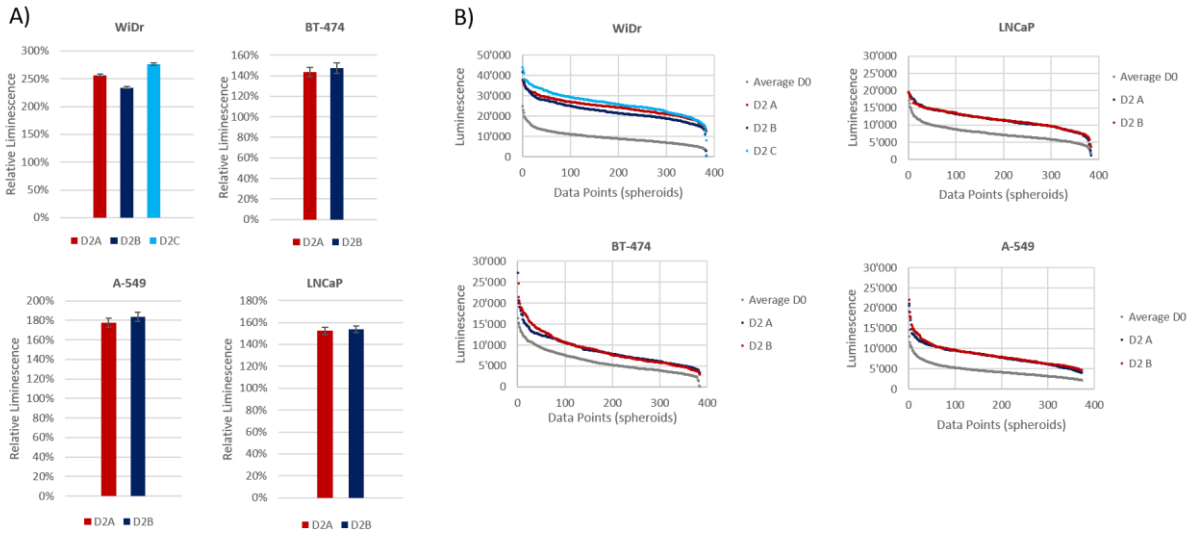

Figure 9: A) Relative luminescence of D2 vs. D0. Tested cell types: WiDr (colon), BT-474 (breast), A-549 (lung), and LNCaP (prostate). Errors indicate SEM. B) Size-sorted luminescence values at D2 and D0. The values from D2 were averages from three (WiDr) or two (BT-474, A-549, LNCaP) 384-well plates, respectively.

would behave similarly and no cell death occurred. Figure 8D indicates that by doing so, all values are above the diagonal red line representing zero culture growth (= stagnation). No values were found below the red line in the area where 3D cultures with negative growth (= cell death) would be expected to localise. Note, however, that this is a mathematical representation. There is no direct biological link between spheroids emitting a small or a large luminescence signal.

Taken together, the viability measurements indicated that there was no unexpected loss of viability.

DISCUSSION

The present study demonstrates how the unique 3D CoSeedis™ platform from abc biopply can be used to grow large quantities of 3D cell cultures for the purpose of HTS. In combination with the COPAS VISION™ instrument from Union Biometrica Inc., we were able to demonstrate a time effective, reliable and unprecedented process to fill 384-well plates with homogenous and uniform 3D spheroids for downstream compound screening. Size distribution of gated and sorted spheroids across one 384-well plate, but also between different 384-well plates, is thereby determined by the preset gating parameters and the precision of the COPAS VISION™. Starting with homogeneous and uniform 3D spheroids in general increases the recovery rate of sorted events and simplifies the entire sorting process. 3D CoSeedis™ therefore plays a major role in making 3D spheroid sorting, and consequently screening, efficient and cost-effective. For example, in the current study, we sorted four to six 384-well plates per cell type with 1 spheroid per well each. In order to collect enough spheroids for sorting, setup and controls, spheroids were harvested from 24 chips (Chip680) corresponding to one 24-well plate. Consequently, we had spheroids in excess and the sorting could be done at a relatively high speed resulting in seeding times of less than 5 minutes per 384-well plate. Such a fast sorting was possible, because the starting spheroid quality was high and spheroids were highly homogenous and available at sufficient

quantities. Lower quality, hence less gated spheroids, and lower quantities of spheroids in suspension result in longer sorting times. Likewise, low quality, i.e. low homogeneity and uniformity of spheroids, will prolong the initial setup time, e.g. optimize gating in order to sort uniform, single spheroids only. Consequently, low quality material of spheroids will increase the required cell culture work substantially, since significantly higher numbers of 3D cell cultures must be generated in order to have sufficient spheroids to be sorted.

Our assessment of cell viability after spheroid sorting also showed that the sorting procedure did no damage to the spheroids. Cell viability assays confirmed that the sorting process in COPAS VISION™ did not induce any detectable cell death. All spheroids performed as expected and showed an increase in viable cells, which correlated with the known doubling times of each particular cell type.

The COPAS VISON™ is able to sort spheroids between 10 to 750 µm. In our setup, we sorted spheroids of approximately 150 - 250 µm in diameter. The cells were aggregated and grown for only 5 to 9 days prior to sorting. Generally, this size is ideal for sorting, however, some cell types would require longer 3D growth periods in order to form more robust and compact spheroids (e.g. HuH-7 and A-549). The principal setup described here, however, is independent of the size of spheroids sorted and the COPAS VISION™ can be used independently of the size of the sorted particles (within the limits indicated above). From the biological point of view, however, it may be desirable to investigate larger spheroidal structures that eventually show a necrotic core and areas of quiescent cells. Those latter cells are of particular interest, for example in cancer research. They define therefore a major target in many anti-cancer compound screens. It is the combination of 3D CoSeedis™'s ability to grow small to large 3D cell structures together with COPAS VISION™'s broad particle sorting range that makes the method presented in this study so revolutionary in HTS.

References

Brandenberg, Nathalie; Hoehnel, Sylke; Kuttler, Fabien; Homicsko, Krisztian; Ceroni, Camilla; Ringel, Till et al. (2020): High-throughput automated organoid culture via stem-cell aggregation in microcavity arrays. In: *Nature biomedical engineering*. DOI: 10.1038/s41551-020-0565-2.

Courau, Tristan; Bonnereau, Julie; Chicoteau, Justine; Bottois, Hugo; Remark, Romain; Assante Miranda, Laura et al. (2019): Cocultures of human colorectal tumor spheroids with immune cells reveal the therapeutic potential of MICA/B and NKG2A targeting for cancer treatment. In: *Journal for immunotherapy of cancer* 7 (1), S. 74. DOI: 10.1186/s40425-019-0553-9.

Das, Viswanath; Fürst, Tomáš; Gurská, Soňa; Džubák, Petr; Hajdúch, Marián (2016): Reproducibility of Uniform Spheroid Formation in 384-Well Plates: The Effect of Medium Evaporation. In: *Journal of biomolecular screening* 21 (9), S. 923–930. DOI: 10.1177/1087057116651867.

Harrer, Stefan; Shah, Pratik; Antony, Bhavna; Hu, Jianying (2019): Artificial Intelligence for Clinical Trial Design. In: *Trends in pharmacological sciences* 40 (8), S. 577–591. DOI: 10.1016/j.tips.2019.05.005.

Kochanek, Stanton J.; Close, David A.; Camarco, Daniel P.; Johnston, Paul A. (2020): Maximizing the Value of Cancer Drug Screening in Multicellular Tumor Spheroid Cultures: A Case Study in Five Head and Neck Squamous Cell Carcinoma Cell Lines. In: *SLAS discovery : advancing life sciences R & D* 25 (4), S. 329–349. DOI: 10.1177/2472555219896999.

Kondo, Jumpei; Ekawa, Tomoya; Endo, Hiroko; Yamazaki, Kanami; Tanaka, Norio; Kukita, Yoji et al. (2019): High-throughput screening in colorectal cancer tissue-originated spheroids. In: *Cancer science* 110 (1), S. 345–355. DOI: 10.1111/cas.13843.

Lee, Jong Min; Park, Da Yeon; Yang, Letao; Kim, Eun-Joong; Ahrberg, Christian D.; Lee, Ki-Bum; Chung, Bong Geun (2018): Generation of uniform-sized multicellular tumor spheroids using hydrogel microwells for advanced drug screening. In: *Scientific reports* 8 (1), S. 17145. DOI: 10.1038/s41598-018-35216-7.

Li, L.; LaBarbera, D. V. (2017): 3D High-Content Screening of Organoids for Drug Discovery. In: Comprehensive Medicinal Chemistry III: Elsevier, S. 388–415.

Ocana, Alberto; Pandiella, Atanasio; Siu, Lillian L.; Tannock, Ian F. (2010): Preclinical development of molecular-targeted agents for cancer. In: *Nature reviews. Clinical oncology* 8 (4), S. 200–209. DOI: 10.1038/nrclinonc.2010.194.

Ryan, Sarah-Louise; Baird, Anne-Marie; Vaz, Gisela; Urquhart, Aaron J.; Senge, Mathias; Richard, Derek J. et al. (2016): Drug Discovery Approaches Utilizing Three-Dimensional Cell Culture. In: *Assay and drug development technologies* 14 (1), S. 19–28. DOI: 10.1089/adt.2015.670.

Thomsen, Andreas R.; Aldrian, Christine; Bronsert, Peter; Thomann, Yi; Nanko, Norbert; Melin, Nicolas et al. (2017): A deep conical agarose microwell array for adhesion independent three-dimensional cell culture and dynamic volume measurement. In: *Lab on a chip* 18 (1), S. 179–189. DOI: 10.1039/c7lc00832e.

Tijmen H. Booij, Leo S. Price, and Erik H. J. Danen: 3D Cell-Based Assays for Drug Screens: Challenges in Imaging, Image Analysis, and High-Content Analysis.

Walzl, Angelika; Unger, Christine; Kramer, Nina; Unterleuthner, Daniela; Scherzer, Martin; Hengstschläger, Markus et al. (2014): The Resazurin Reduction Assay Can Distinguish Cytotoxic from Cytostatic Compounds in Spheroid Screening Assays. In: *Journal of biomolecular screening* 19 (7), S. 1047–1059. DOI: 10.1177/1087057114532352.